

1 • **Stratospheric Chemistry**

---

2

3

4

5 **Chapter 6 Supplementary Material**

6

7 **Includes:**

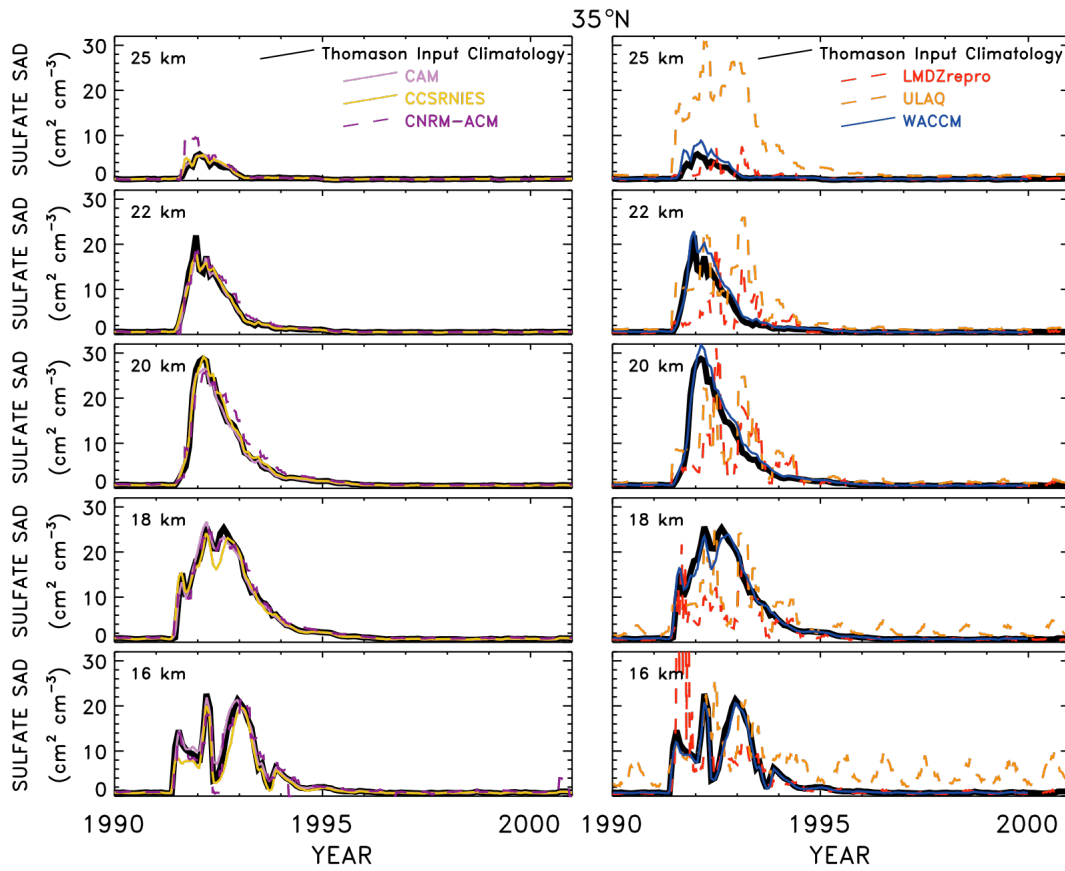
8 • 6S Supplementary Figures (6S-1 through 6S-20)

9 • 6S Tables (6S-1 through 6S-4)

10 • Photocomp 2008 Experiment

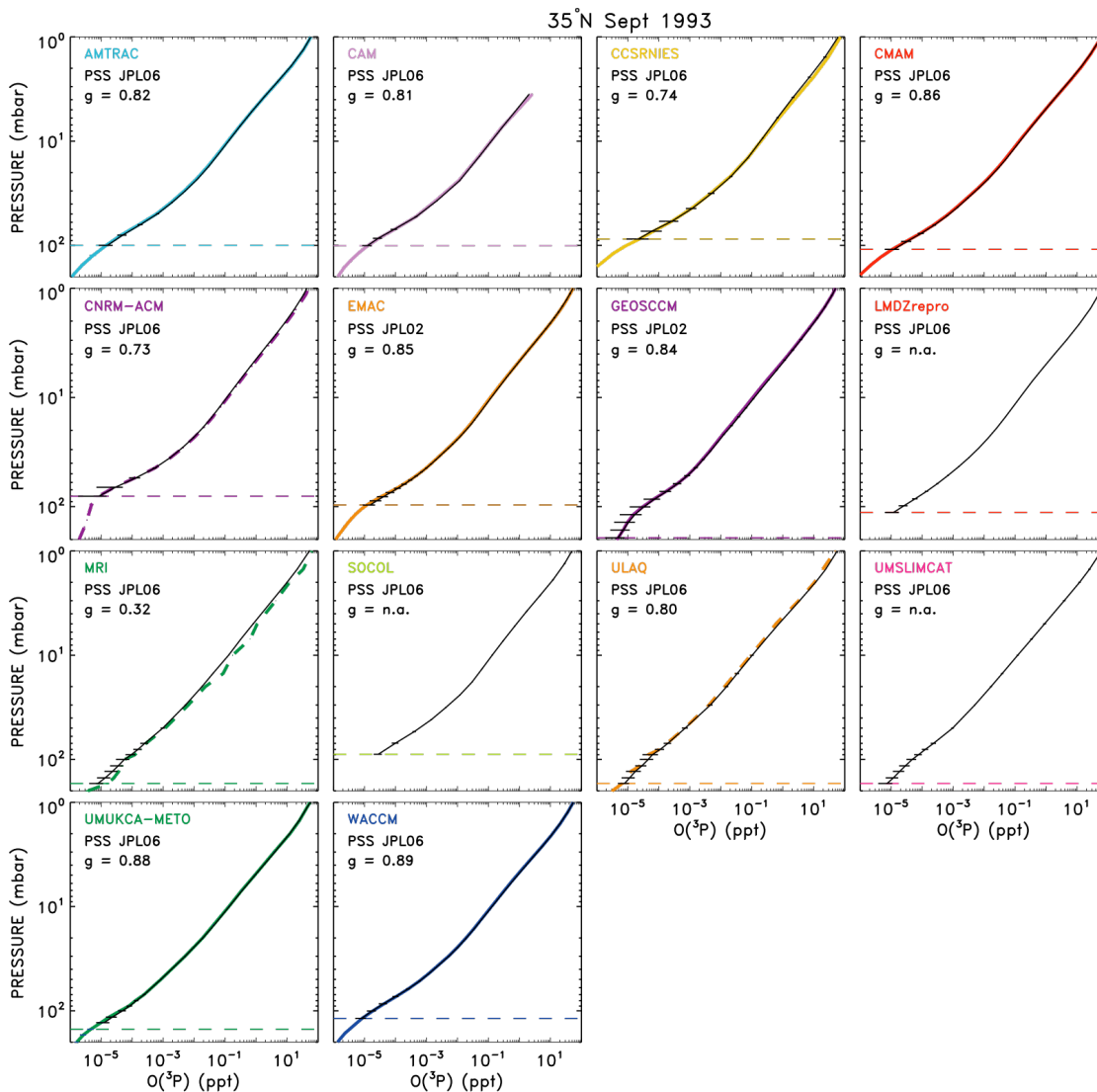
11

12 **6S Supplemental Figures**

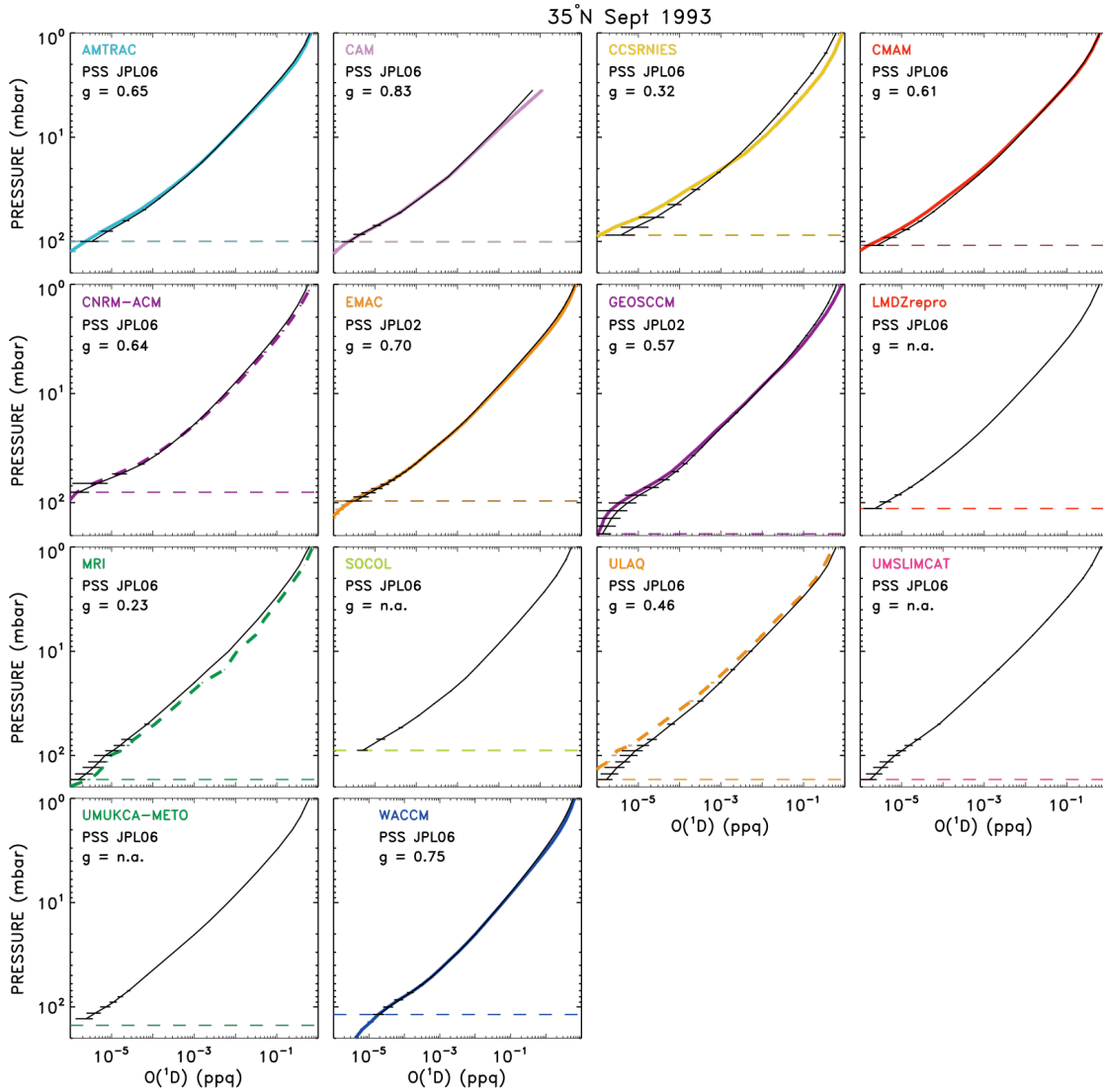


13

14 **Figure 6S-1:** Sulfate surface area density ( $\text{cm}^2 \text{cm}^{-3}$ ) time series at  $35^\circ\text{N}$  and 25km,  
15 22km, 20km, 18km, and 16km for CAM3.5, CCSRNIES, CNRM-ACM, LMDZrepro,  
16 ULAQ, and WACCM.

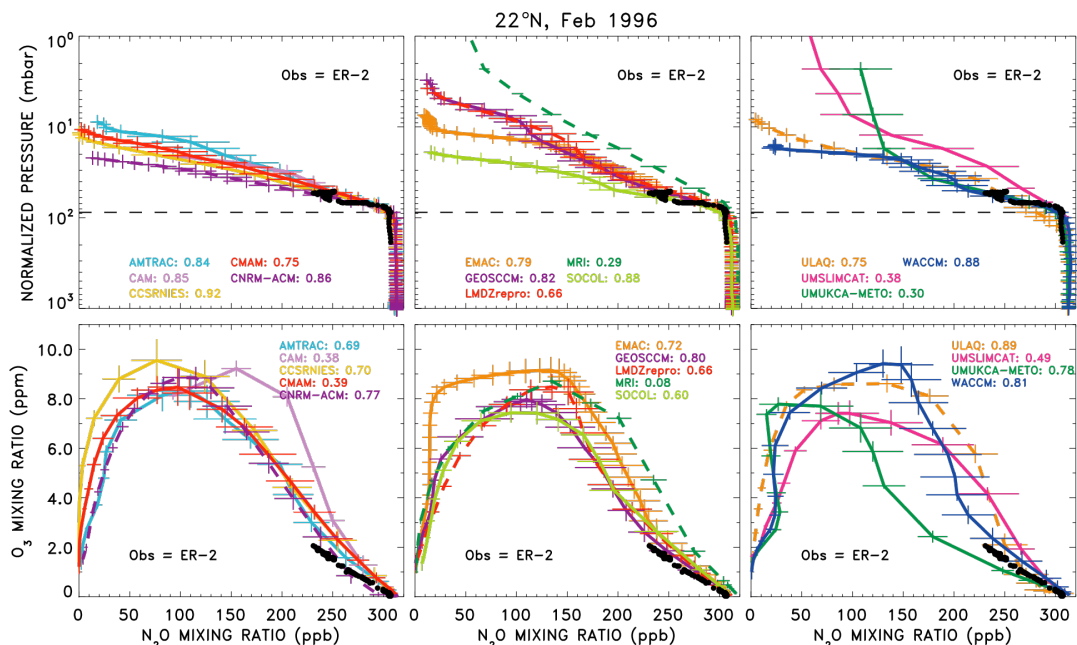


17  
 18 **Figure 6S-2a:** Comparison of zonal, monthly mean profiles of  $O(^3P)$  radicals from CCM  
 19 models (coloured lines and symbols) versus 24-hour average radical profiles found using  
 20 a PSS box model constrained by profiles of T,  $O_3$ ,  $H_2O$ ,  $CH_4$ , CO,  $NO_Y$ ,  $Cl_Y$ ,  $Br_Y$ , and  
 21 sulfate SAD from the various CCMs for 35°N in **September 1993**. The PSS model was  
 22 run for CCM model levels from the tropopause (dashed lines) to 1 hPa. The PSS model  
 23 uses the latitude of the CCM output that is closest to 35°N and solar declination  
 24 corresponding to the mid point of the monthly mean. Numerical values of g and the  
 25 chemical kinetics in the simulation are given (see main chapter text). The coloured error  
 26 bars represent the standard deviation about the zonal monthly mean for various days used  
 27 to compute the mean. The black error bars represent the sensitivity of PSS output to  
 28 variability in the CCM profiles of radical precursors.  
 29

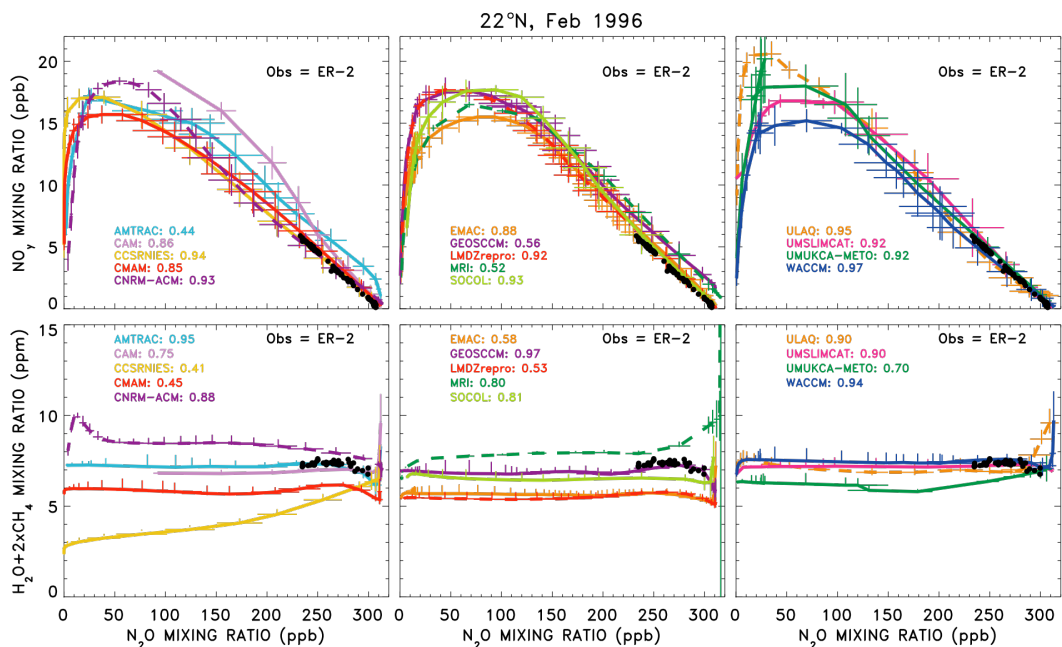


30  
31  
32

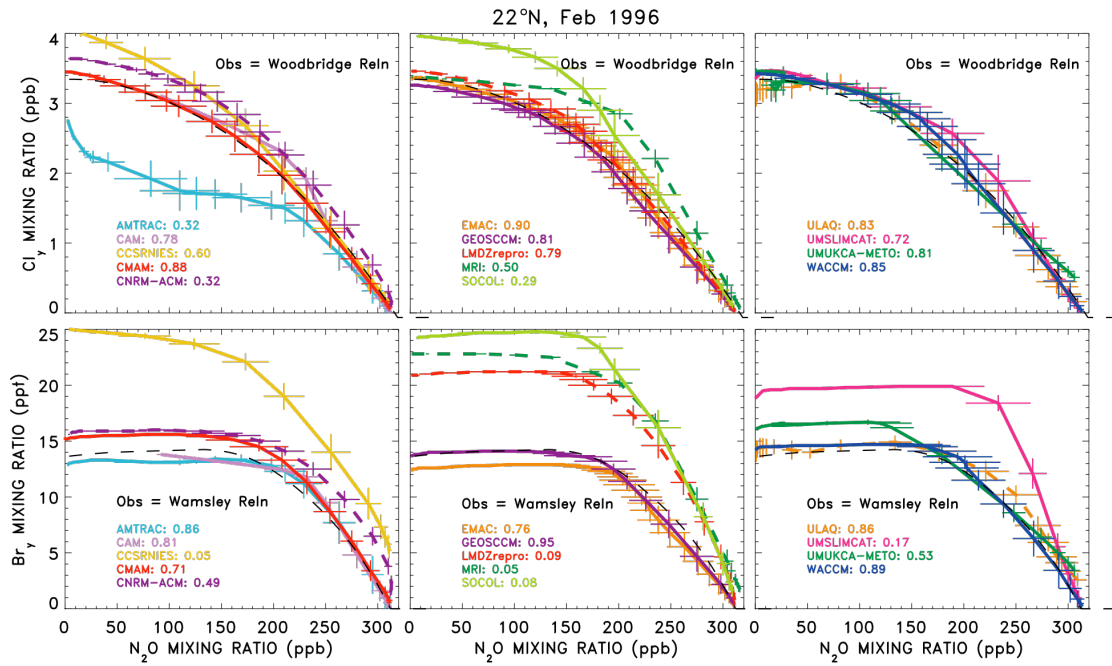
Figure 6S-2b: same as Figure 6S-2a, except  $O(^1D)$  is shown.



33  
34 **Figure 6S-3a:** Comparison of N<sub>2</sub>O profile and the relation of radical precursors versus  
35 N<sub>2</sub>O (black) to zonal, monthly mean values from various CCM models (coloured lines  
36 and symbols, as indicated) for **February 1996**. CCM output is for the closest model  
37 latitude to 22°N, as indicated. Numerical values of g (see main chapter text) are also  
38 noted. Comparisons of N<sub>2</sub>O vs pressure and O<sub>3</sub> vs N<sub>2</sub>O are shown.

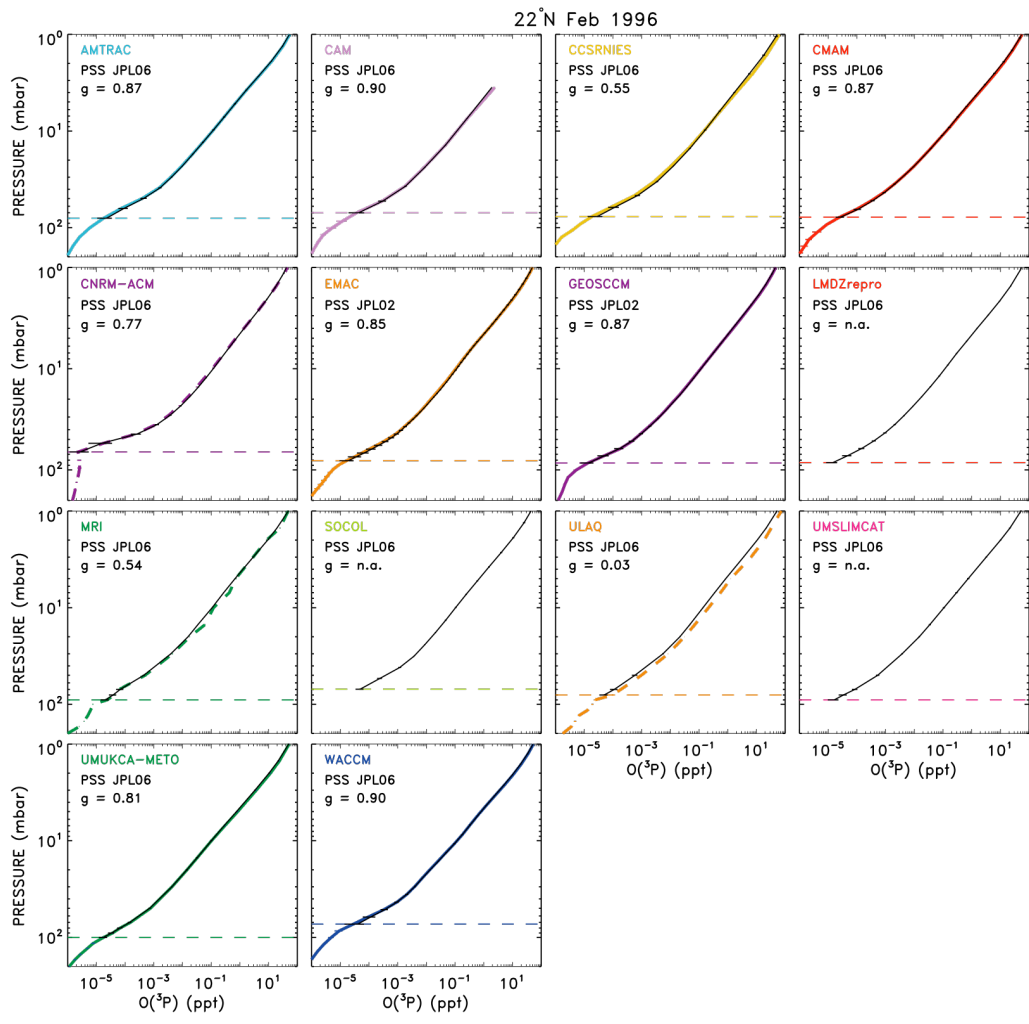


39  
40 **Figure 6S-3b:** Same as Figure 6S-3a, except comparisons of NO<sub>Y</sub> vs N<sub>2</sub>O and  
41 H<sub>2</sub>O+2×CH<sub>4</sub> vs N<sub>2</sub>O are shown.



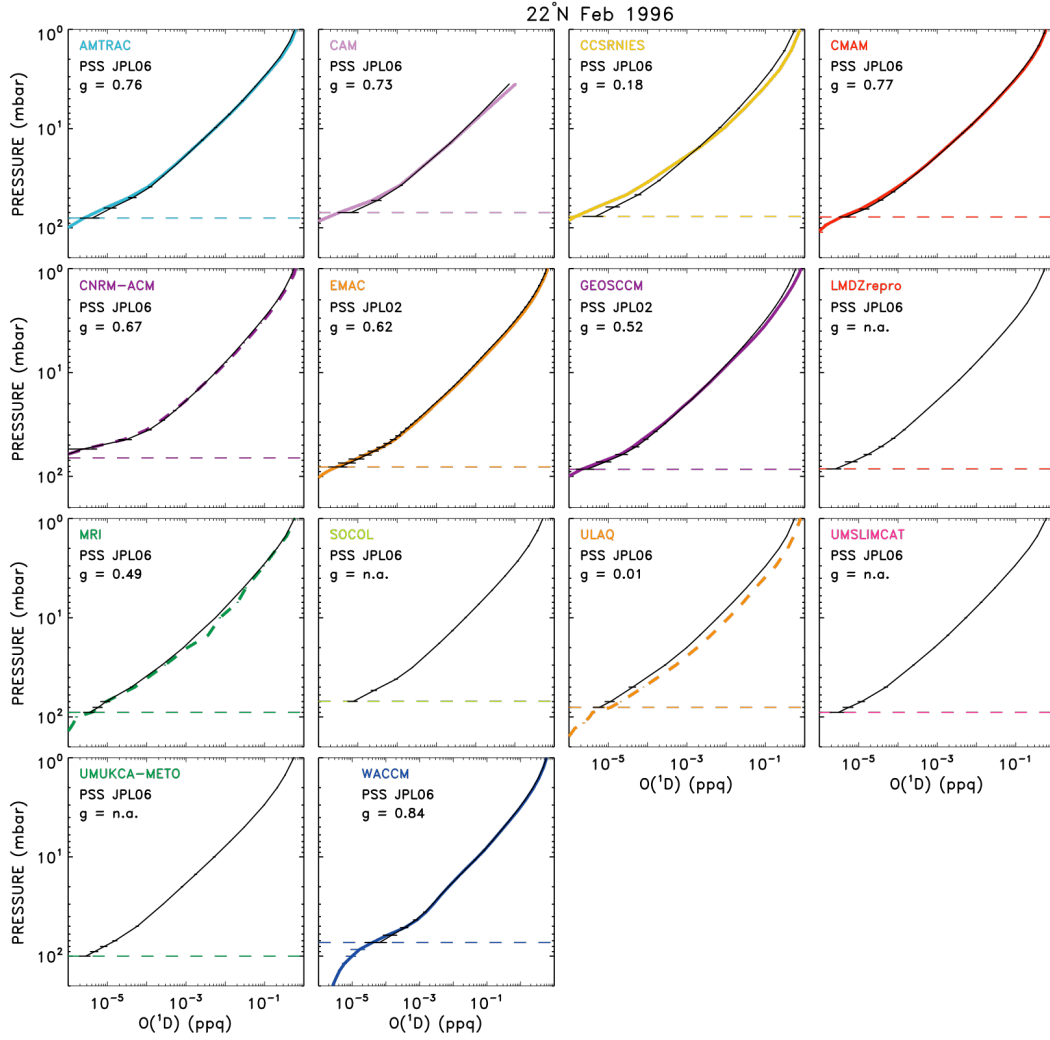
42  
43  
44  
45

**Figure 6S-3c:** same as Figure 6S-3a, except comparisons of  $Cl_Y$  vs  $N_2O$  and  $Br_Y$  vs  $N_2O$  are shown.



46  
 47  
 48  
 49  
 50  
 51  
 52  
 53  
 54  
 55  
 56  
 57  
 58

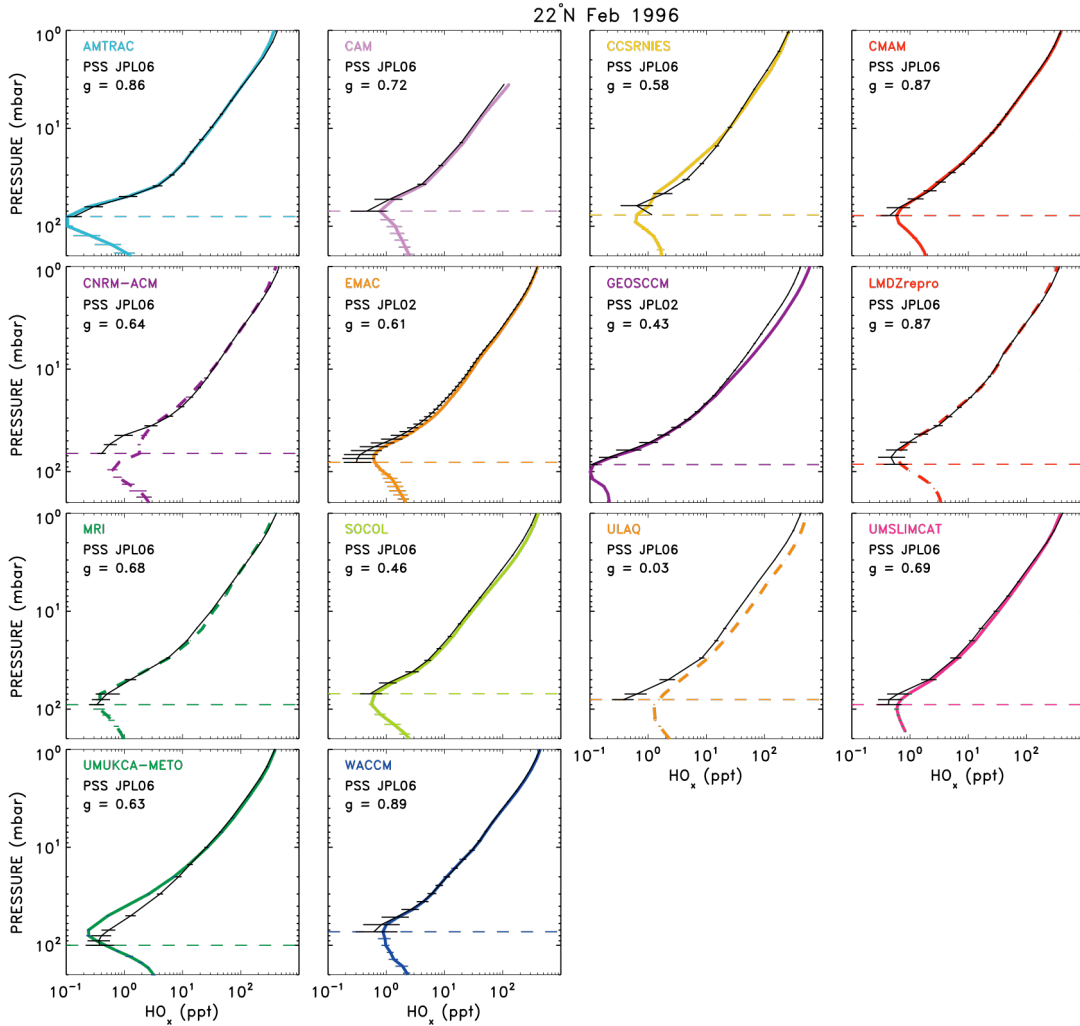
**Figure 6S-4a:** Comparison of zonal, monthly mean profiles of  $O(^3P)$  radicals from CCM models (coloured lines and symbols) versus 24-hour average radical profiles found using a PSS box model constrained by profiles of T,  $O_3$ ,  $H_2O$ ,  $CH_4$ , CO,  $NO_Y$ ,  $Cl_Y$ ,  $Br_Y$ , and sulfate SAD from the various CCMs for  $22^\circ N$  in **February 1996**. The PSS model was run for CCM model levels from the tropopause (dashed lines) to 1 hPa. The PSS model uses the latitude of the CCM output that is closest to  $22^\circ N$  and solar declination corresponding to the mid point of the monthly mean. Numerical values of g and the chemical kinetics in the simulation are given (see main chapter text). The coloured error bars represent the standard deviation about the zonal monthly mean for various days used to compute the mean. The black error bars represent the sensitivity of PSS output to variability in the CCM profiles of radical precursors.



59  
60

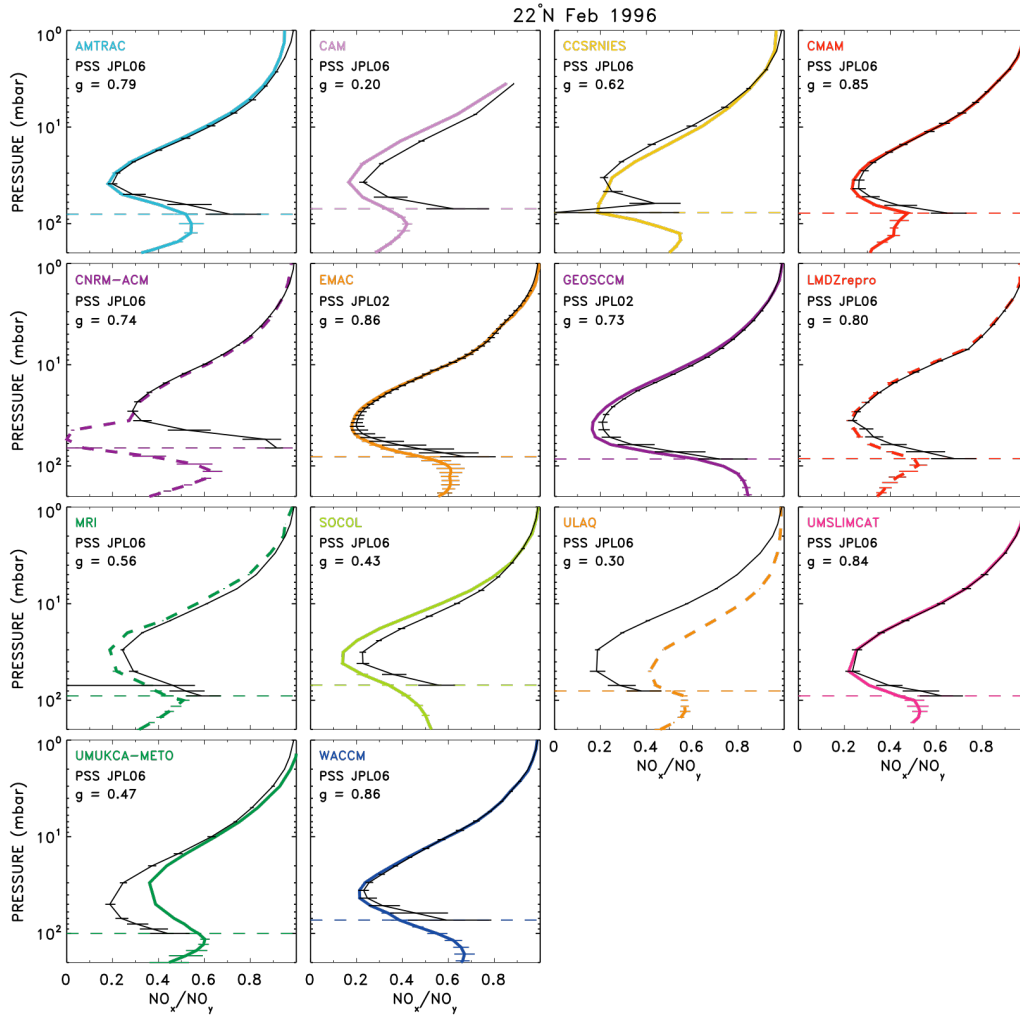
Figure 6S-4b: same as Figure 6S-4a, except  $O(^1D)$  is shown.





61  
62

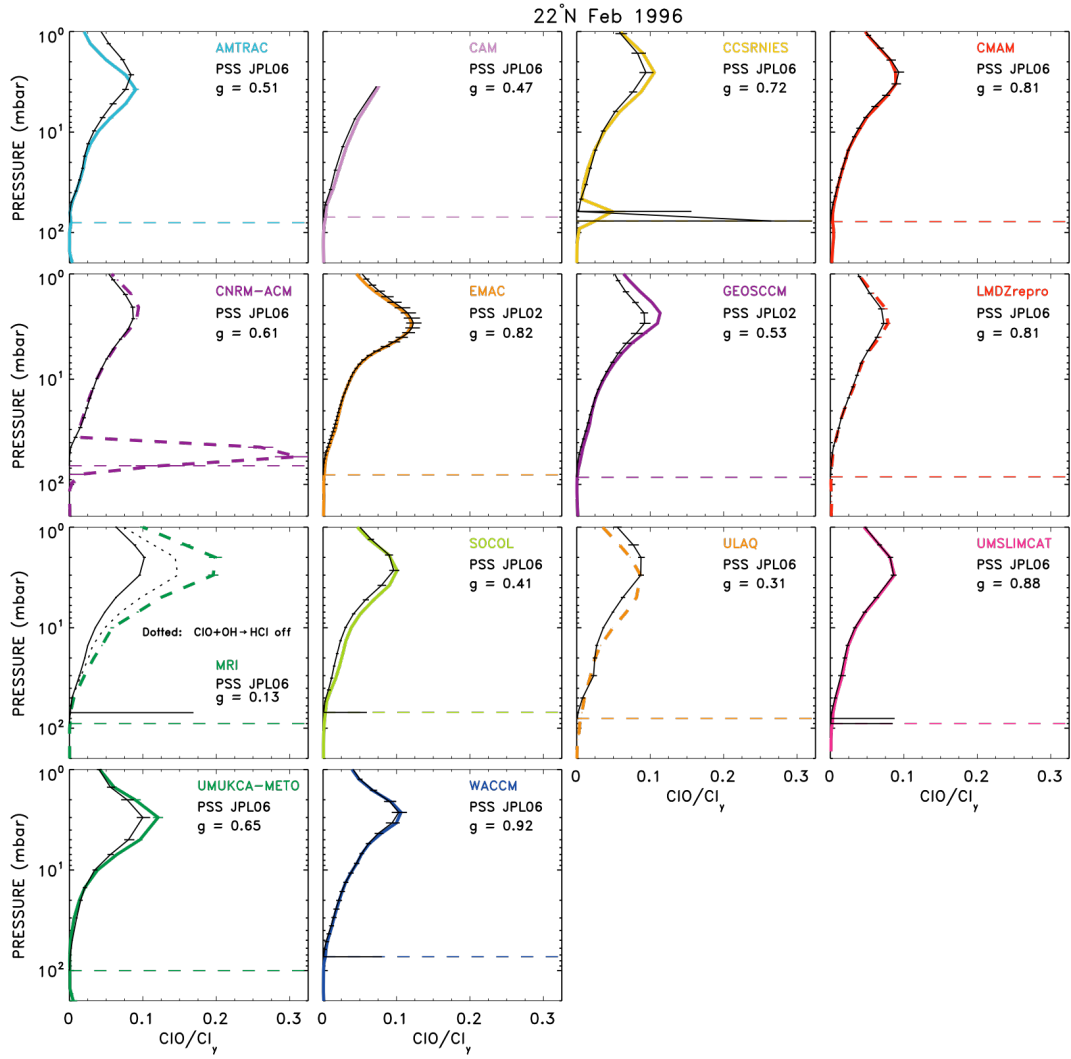
Figure 6S-4c: same as Figure 6S-4a, except  $\text{HO}_x$  is shown.



63

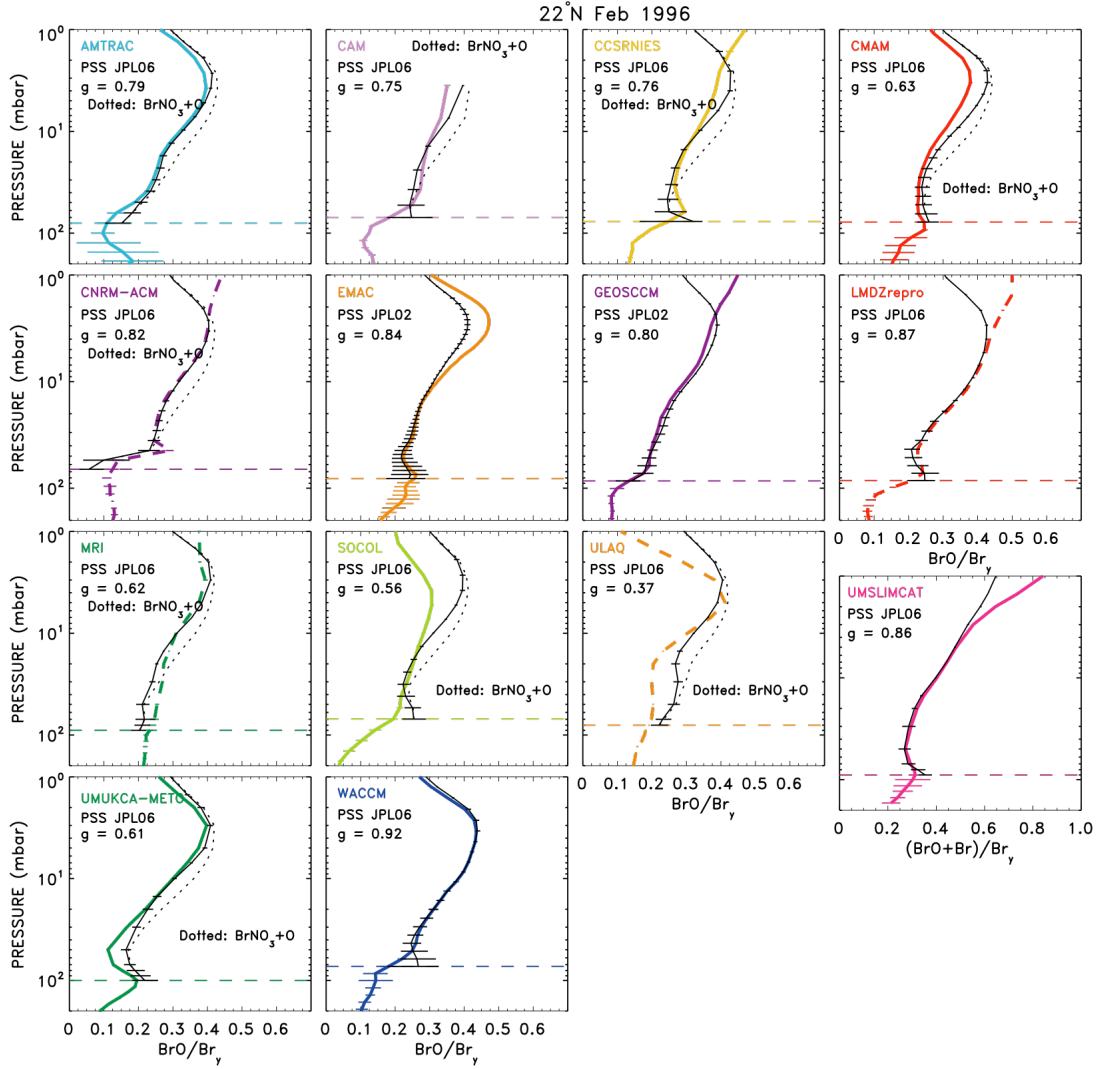
64

Figure 6S-4d: same as Figure 6S-4a, except NO<sub>x</sub>/NO<sub>y</sub> is shown.



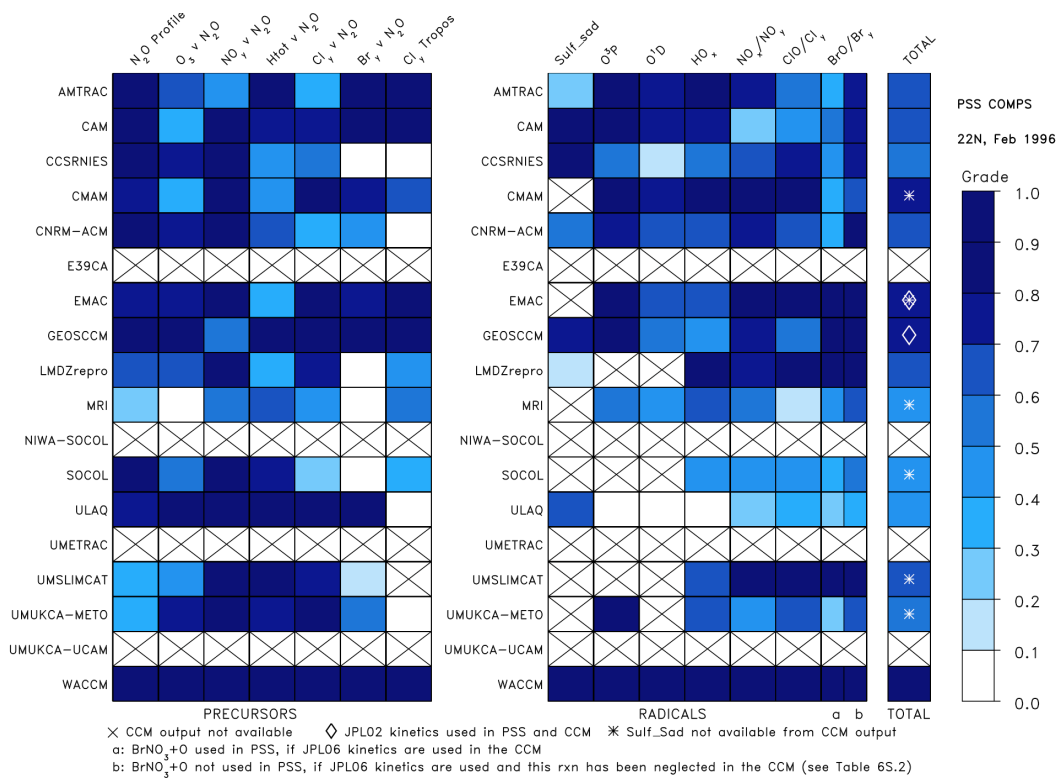
65  
66

Figure 6S-4e: same as Figure 6S-4a, except  $\text{ClO}/\text{Cl}_y$  is shown.



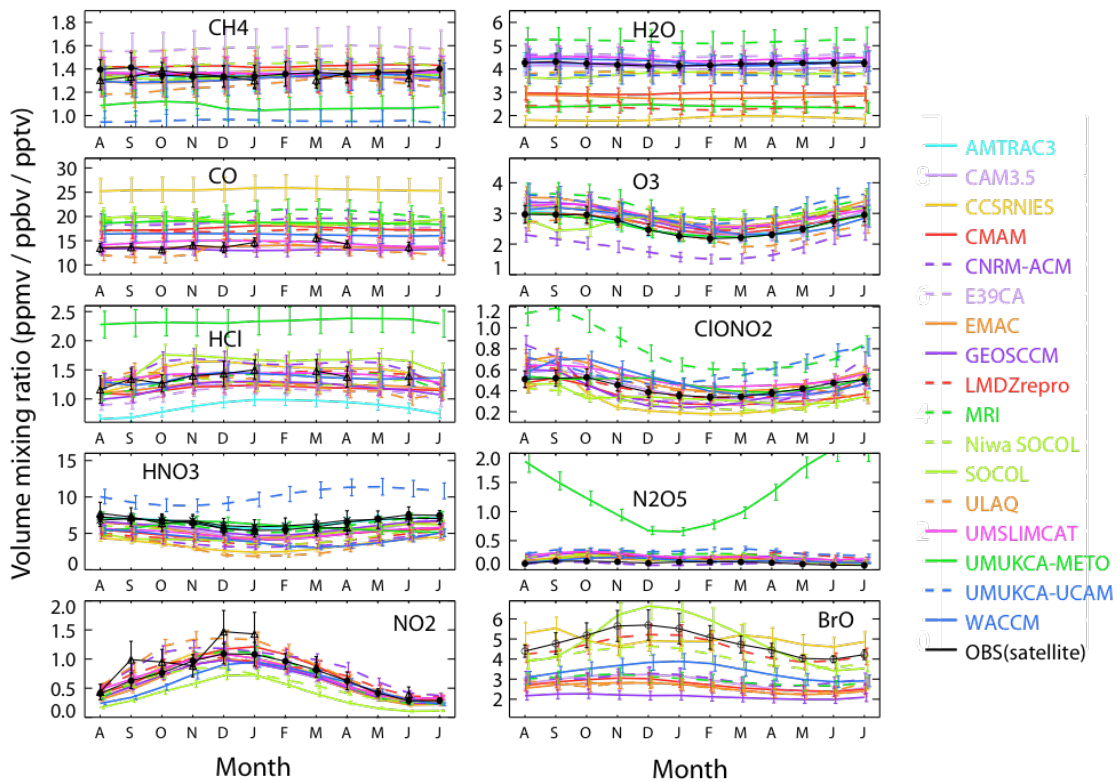
67  
68

Figure 6S-4f: same as Figure 6S-4a, except  $\text{BrO}/\text{Br}_y$  is shown.

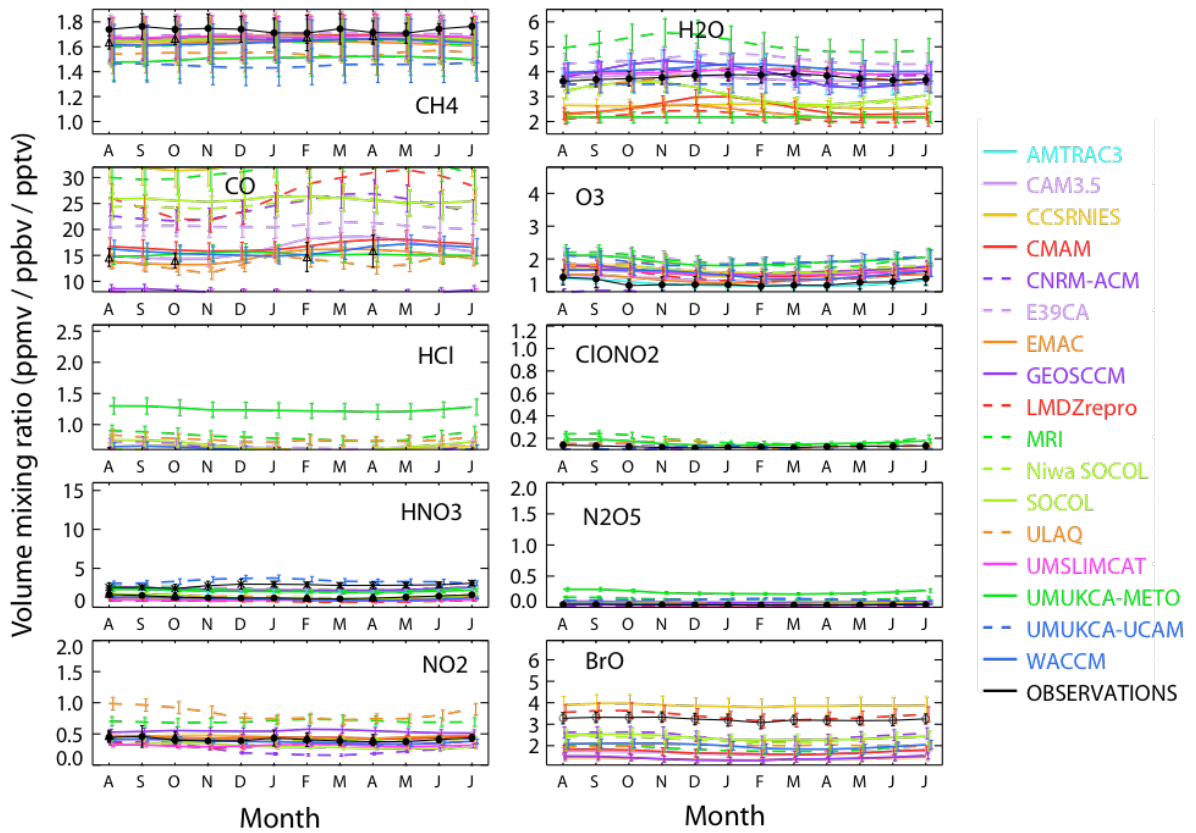


69  
70  
71  
72  
73  
74  
75  
76  
77  
78

**Figure S6-5:** Metrics for (a, left) radical precursors and (b, right) sulfate surface area and radicals for a simulation carried out at 22°N February 1996. The same dark shade of blue is used for  $0.8 < g < 1.0$ , reflecting that there is little significance in differences that fall within this range of values. The symbol X denotes CCM output not archived; ◇ denotes use of JPL-2002 kinetics, and \* denotes sulfate SAD not archived (see main chapter text). For models that used JPL-2006 kinetics and neglected the BrONO<sub>2</sub>+O reaction, two grades are given for the evaluation of BrO/Br<sub>1</sub> (see text).

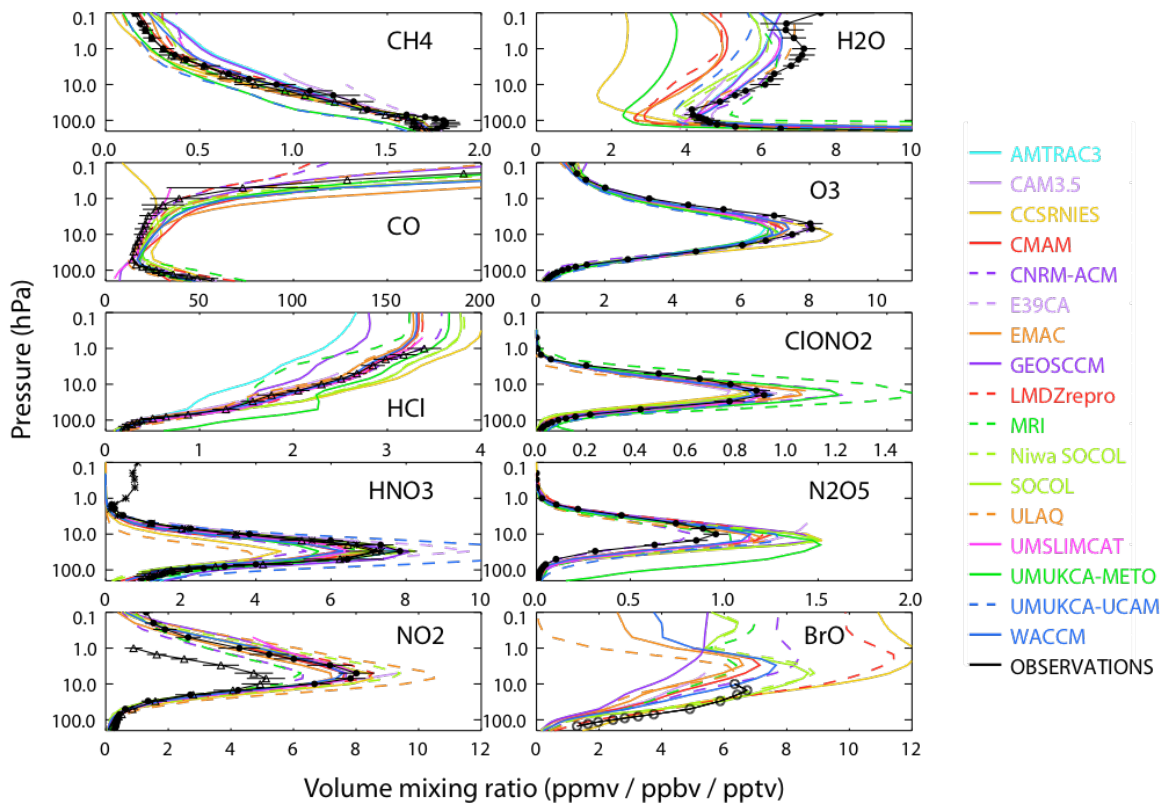


79  
 80 **Figure 6S-6:** Mean annual cycle for 30°S-60°S at 50 hPa for modelled (a) CH<sub>4</sub>, (ppmv)  
 81 (b) H<sub>2</sub>O (ppmv), (c) CO (ppbv), (d) O<sub>3</sub> (ppmv), (e) HCl (ppbv), (f) ClONO<sub>2</sub> (ppbv), (g)  
 82 HNO<sub>3</sub> (ppbv), (h) N<sub>2</sub>O<sub>5</sub> (ppbv), (i) NO<sub>2</sub> (ppbv) and (j) BrO (pptv). The CCM data is  
 83 taken from the T2Mz files (2000-2004, except E39CA model 1996-2000). Also shown  
 84 are corresponding satellite observations from MIPAS (CH<sub>4</sub>, H<sub>2</sub>O, O<sub>3</sub>, ClONO<sub>2</sub>, HNO<sub>3</sub>,  
 85 N<sub>2</sub>O<sub>5</sub>, NO<sub>2</sub>), ACE (CO, HCl), ODIN (HNO<sub>3</sub>) and SCIAMACHY (BrO). The error bars  
 86 are the standard deviations in the monthly mean values (except for ACE data).



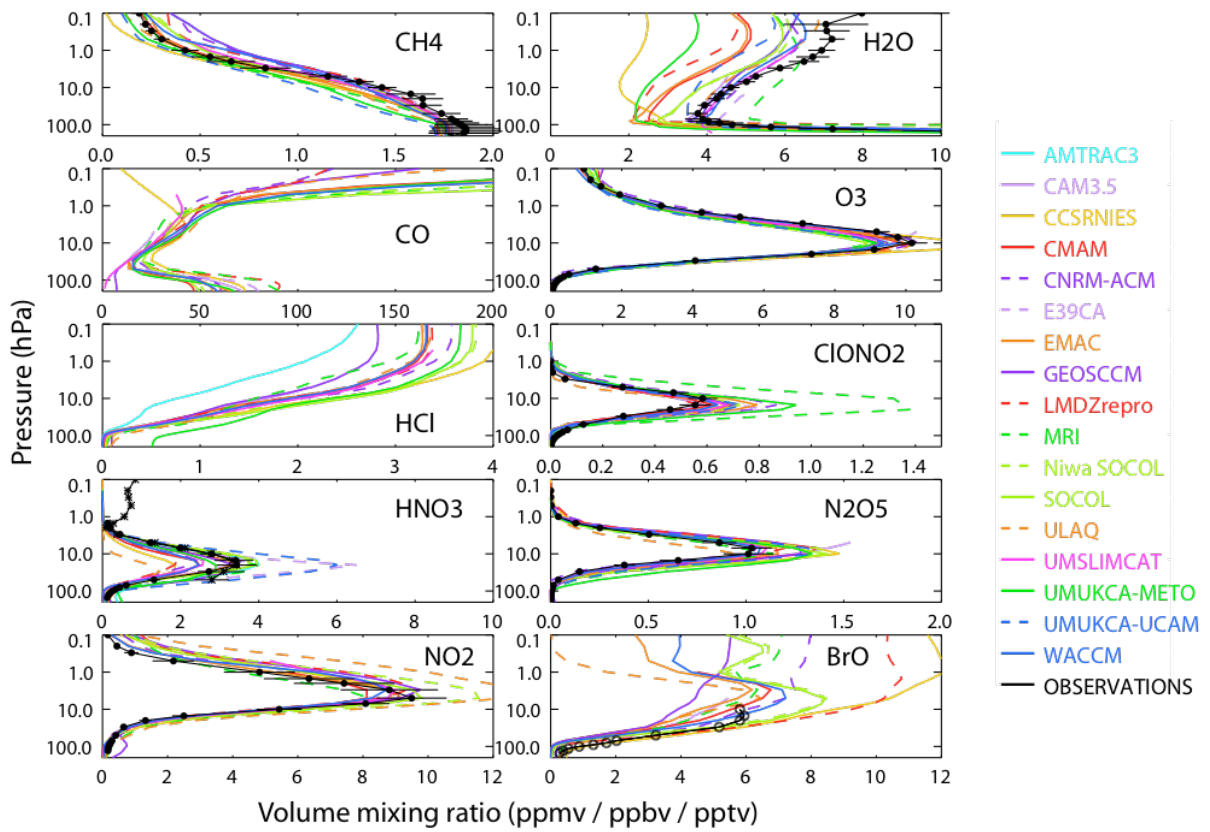
87  
88  
89

**Figure 6S-7:** As Figure 6S-6 but for the tropics 30°S-30°N.

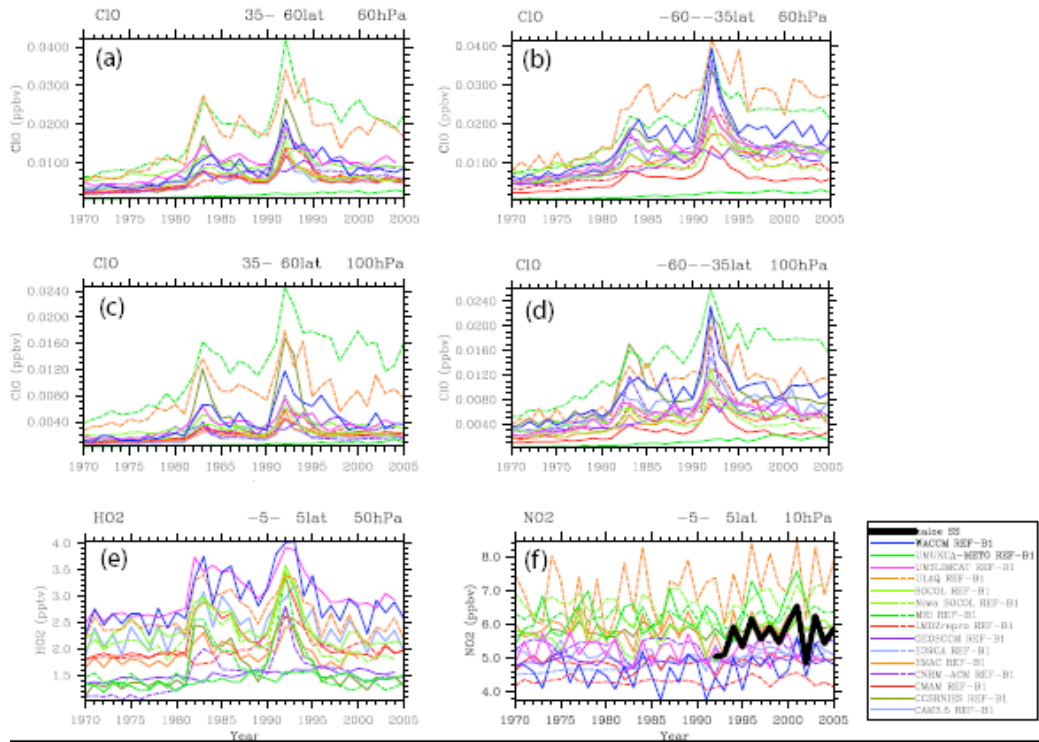


90  
 91 **Figure 6S-8:** Mean profiles for 30°N-60°N for modelled (a) CH<sub>4</sub>, (ppmv) (b) H<sub>2</sub>O  
 92 (ppmv), (c) CO (ppbv), (d) O<sub>3</sub> (ppmv), (e) HCl (ppbv), (f) ClONO<sub>2</sub> (ppbv), (g) HNO<sub>3</sub>  
 93 (ppbv), (h) N<sub>2</sub>O<sub>5</sub> (ppbv), (i) NO<sub>2</sub> (ppbv) and (j) BrO (pptv). The CCM data is taken from  
 94 the T2Mz files (2000-2004, except E39CA model 1996-2000). Also shown are  
 95 corresponding satellite observations from MIPAS (CH<sub>4</sub>, H<sub>2</sub>O, O<sub>3</sub>, ClONO<sub>2</sub>, HNO<sub>3</sub>, N<sub>2</sub>O<sub>5</sub>,  
 96 NO<sub>2</sub>), ACE (CO, HCl), ODIN (HNO<sub>3</sub>) and SCIAMACHY (BrO). The error bars are the  
 97 standard deviations in the annual mean values (except for ACE data).  
 98



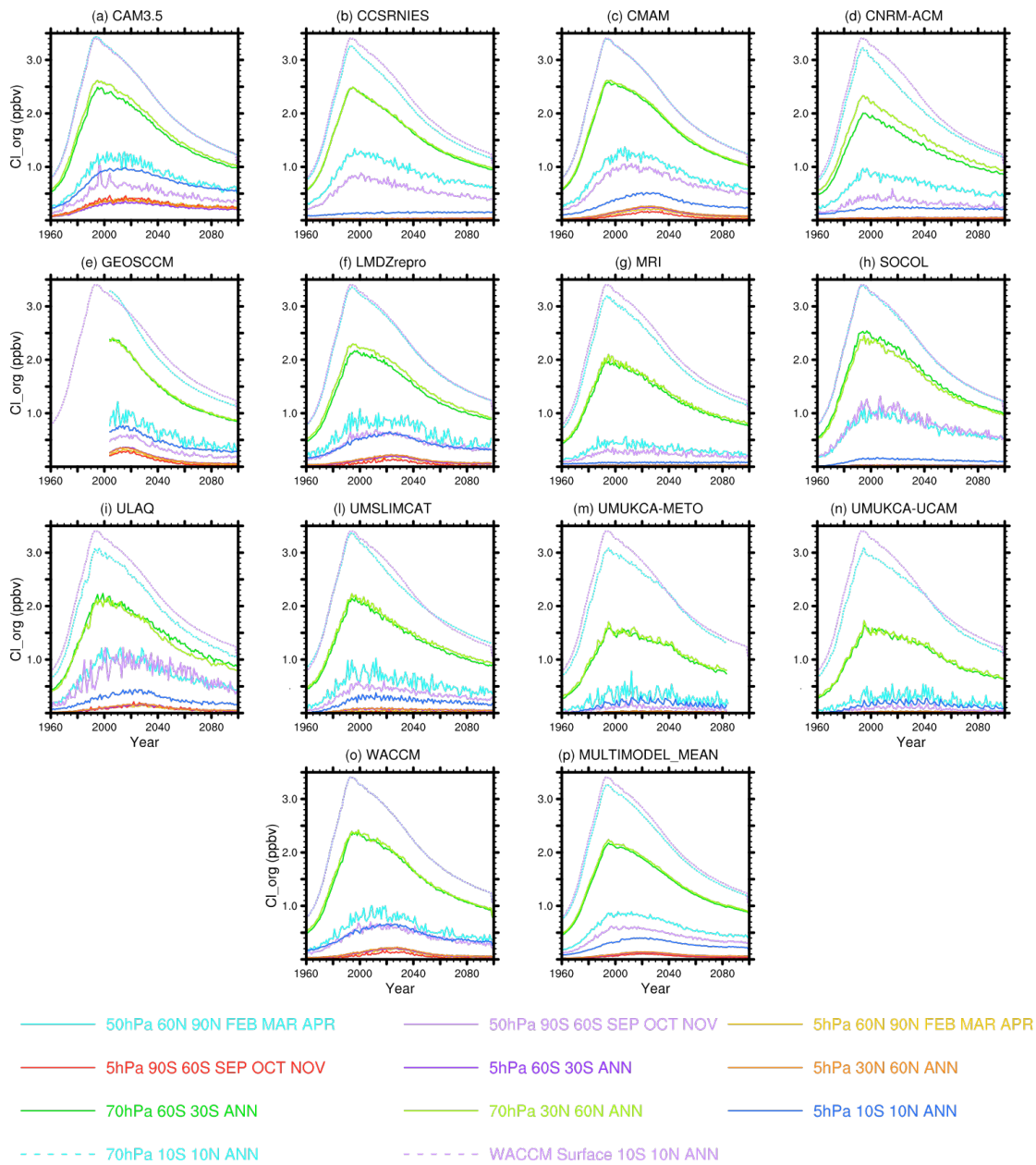


99  
 100 **Figure 6S-9:** As Figure 6S-8 but for the tropics 30°S-30°N.  
 101  
 102



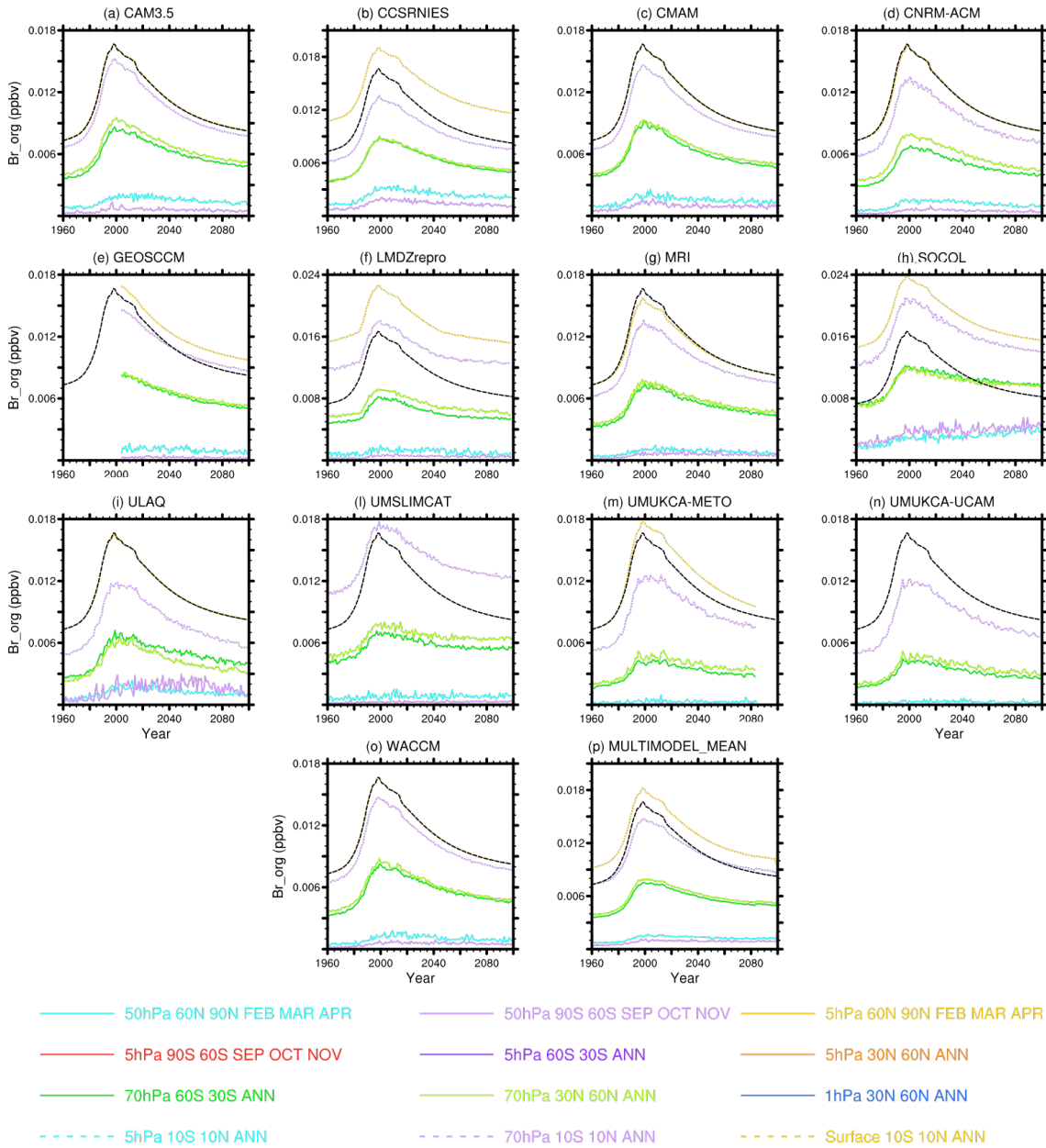
103  
 104  
 105  
 106  
 107  
 108  
 109  
 110  
 111  
 112

**Figure 6S-10.** Time series of mean tracer mixing ratios for (a) CIO (ppbv) 35°N-60°N at 60 hPa, (b) CIO (ppbv) 35°S-60°S at 60 hPa, (c) CIO (ppbv) 35°N-60°N at 100 hPa, (d) CIO (ppbv) 35°S-60°S at 100 hPa, (e) HO<sub>2</sub> (pptv) 5°S-5°N at 50 hPa, and (f) NO<sub>2</sub> (ppbv) 5°S-5°N at 10 hPa. Also shown for NO<sub>2</sub> are HALOE sunset observations converted to 24-hr mean using output from the EMAC model.



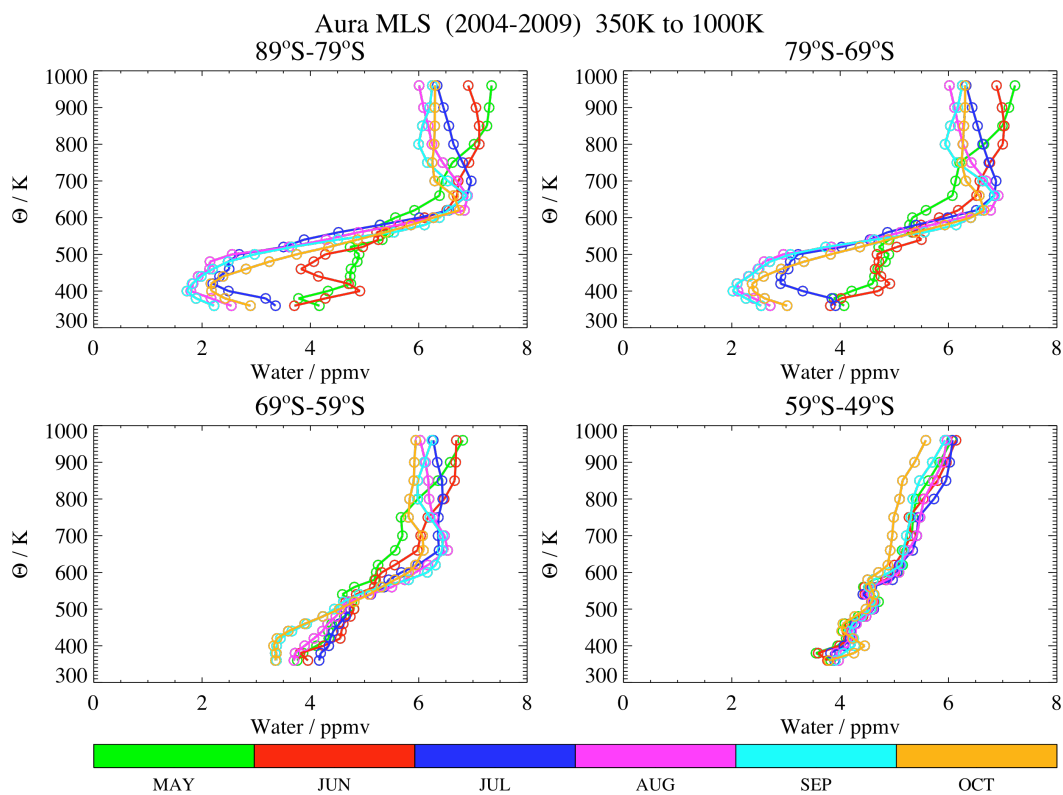
113  
 114  
 115  
 116  
 117  
 118  
 119  
 120  
 121

**Figure 6S-11:** Time series of organic chlorine volume mixing ratio (organic chlorine tracers) (ppbv) from 1960 to 2100 from 13 **REF-B2** CCM simulations and the multimodel mean. A selection of averages within different latitude bands and at different altitudes are plotted. For reference, each panel also includes the total chlorine curve from the WACCM model at the surface (black dashed line).



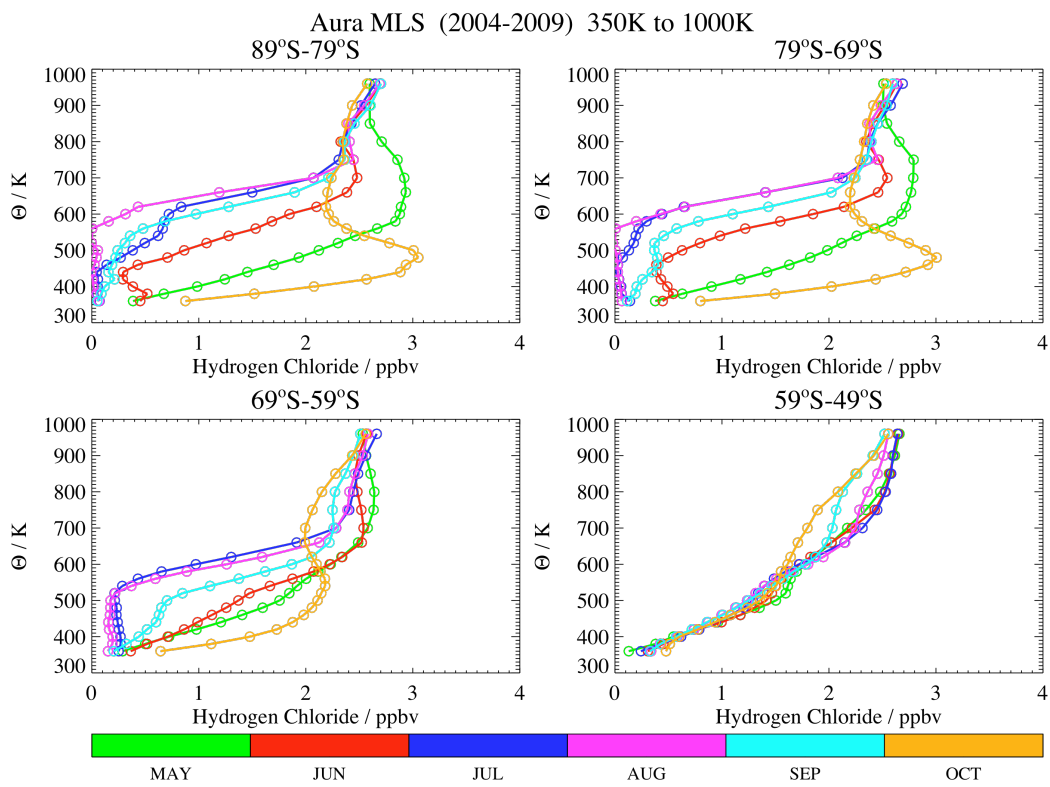
122  
 123  
 124  
 125

Figure 6S-12: As Figure 6S-11 but for organic bromine mixing ratio (pptv).



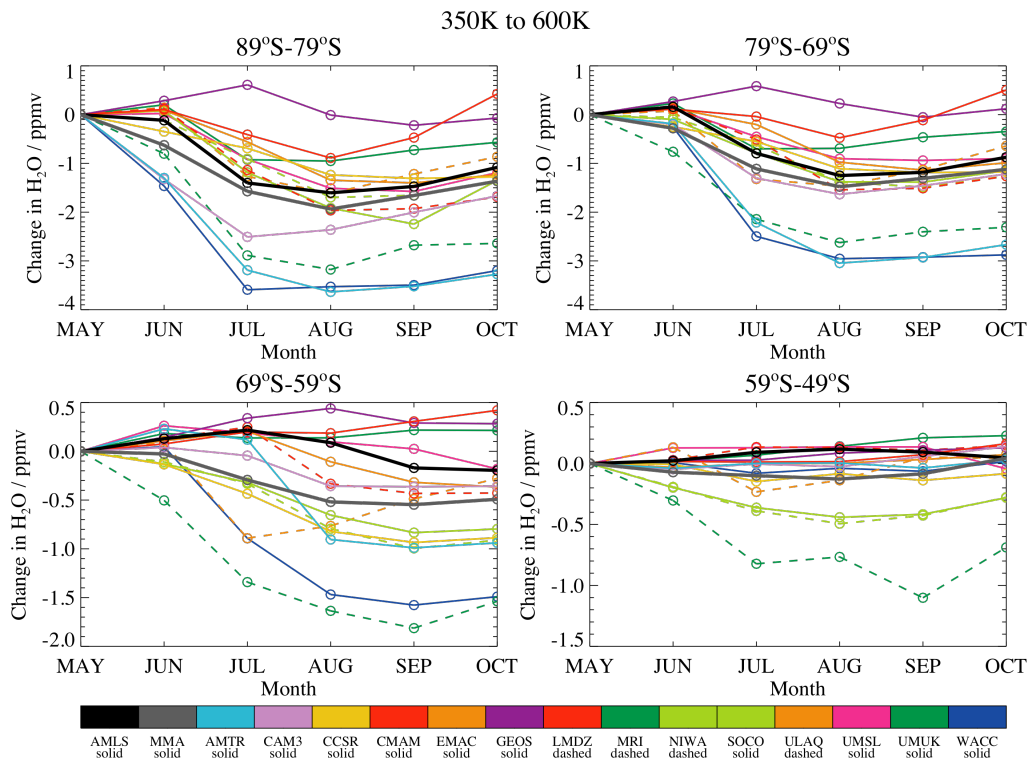
126  
127  
128  
129  
130  
131

**Figure 6S-13.** Southern hemisphere profiles of H<sub>2</sub>O versus  $\theta$  from Aura MLS at mid-month (on the 15<sup>th</sup> day of each month shown in colour bar), from May through October, based on a 5-yr MLS climatology (mid-2004 to mid-2009). Profiles are averaged over the EqL ranges shown above each panel.



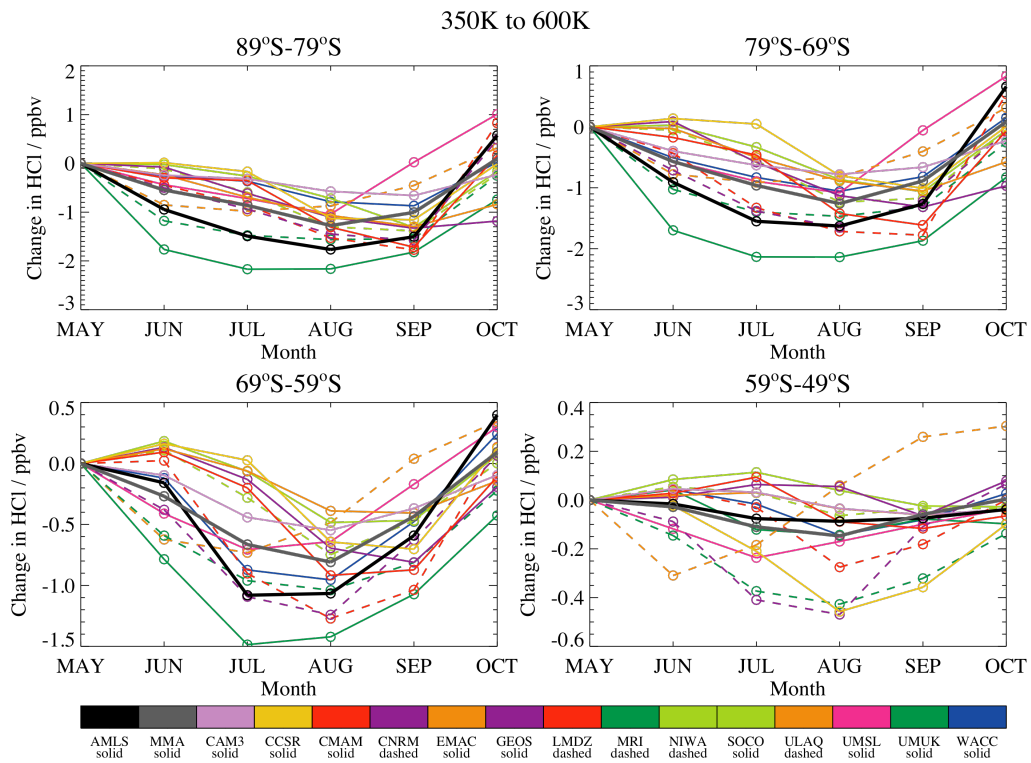
132  
133

**Figure 6S-14.** Same as Figure 6S-13, except for HCl.



134  
135  
136  
137  
138

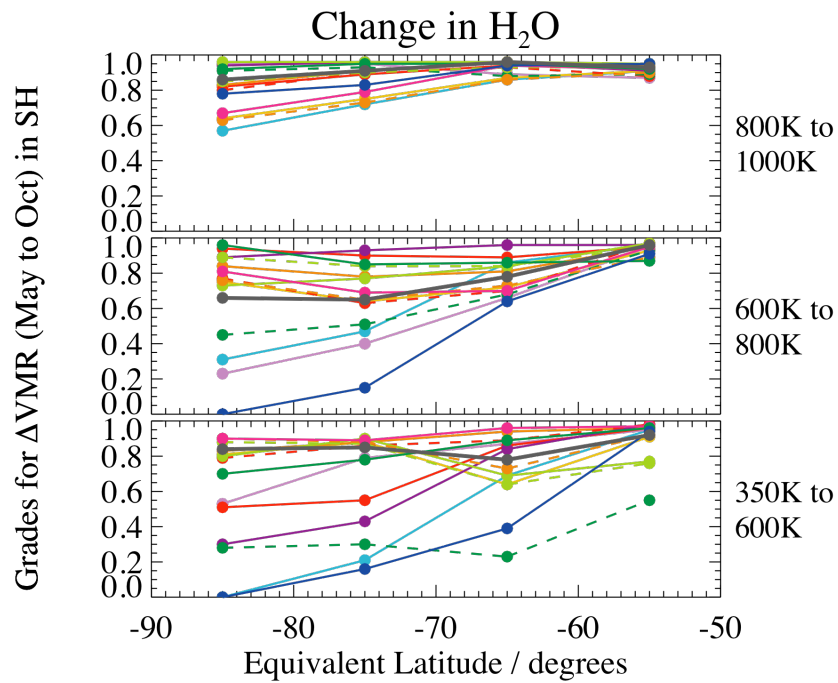
**Figure 6S-15:** Change in H<sub>2</sub>O from 350K to 600K, relative to May, for Aura MLS (abbreviated as AMLS in legend) and 14 CCM climatologies (legend uses first 4 letters of each model) and multimodel mean.



139  
140  
141

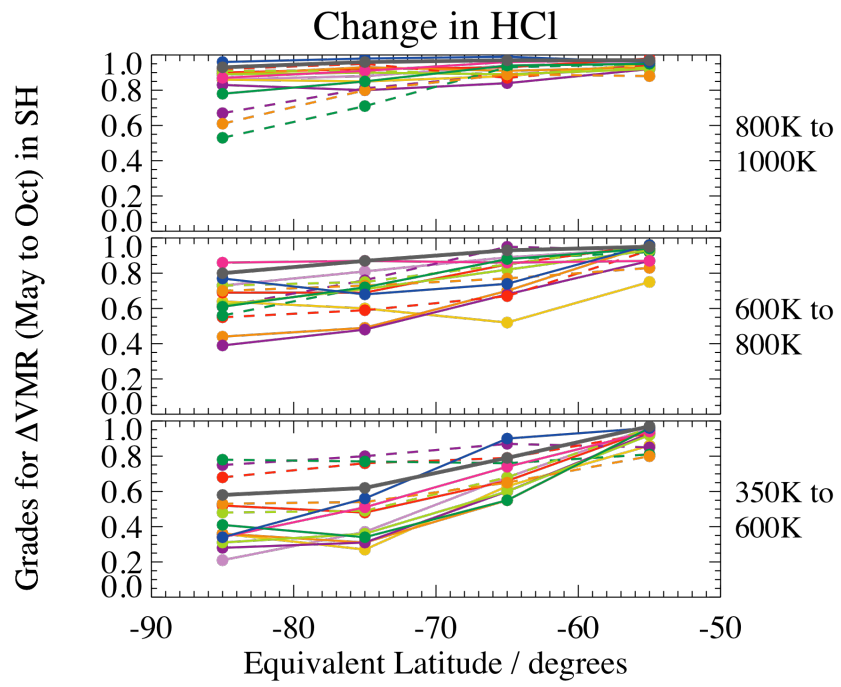
**Figure 6S-16:** As Figure 6S-15 but for HCl.





142  
 143  
 144  
 145  
 146  
 147

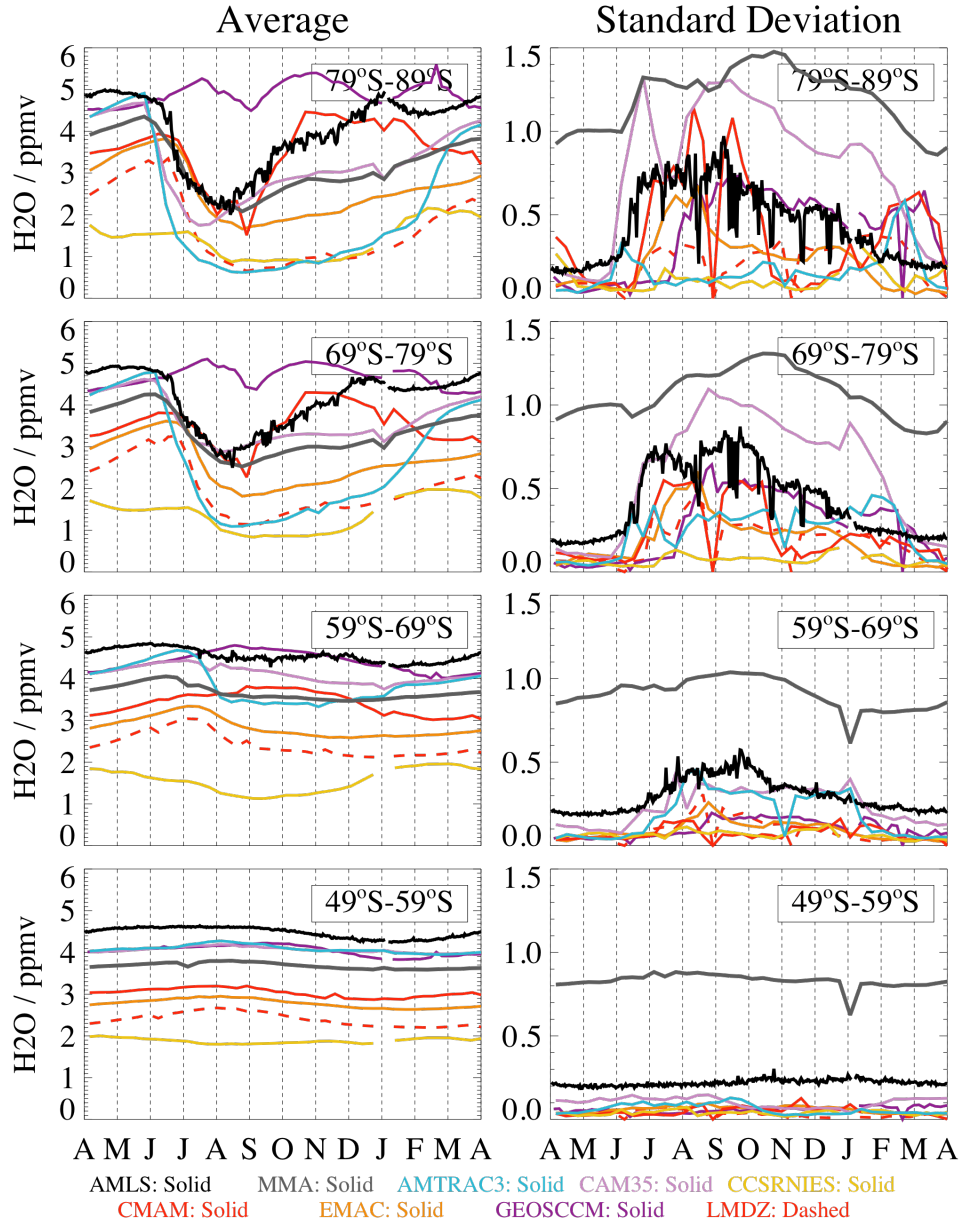
**Figure 6S-17:** Grades obtained for 14 CCMs from a comparison of model versus MLS-derived climatological changes in H<sub>2</sub>O (see main chapter text and Figure 6S-12). Grades are calculated for 4 EqL bins and 3 ranges of  $\theta$  values. Colours and linestyles correspond to those shown in Figure 6S-16.



148  
149  
150

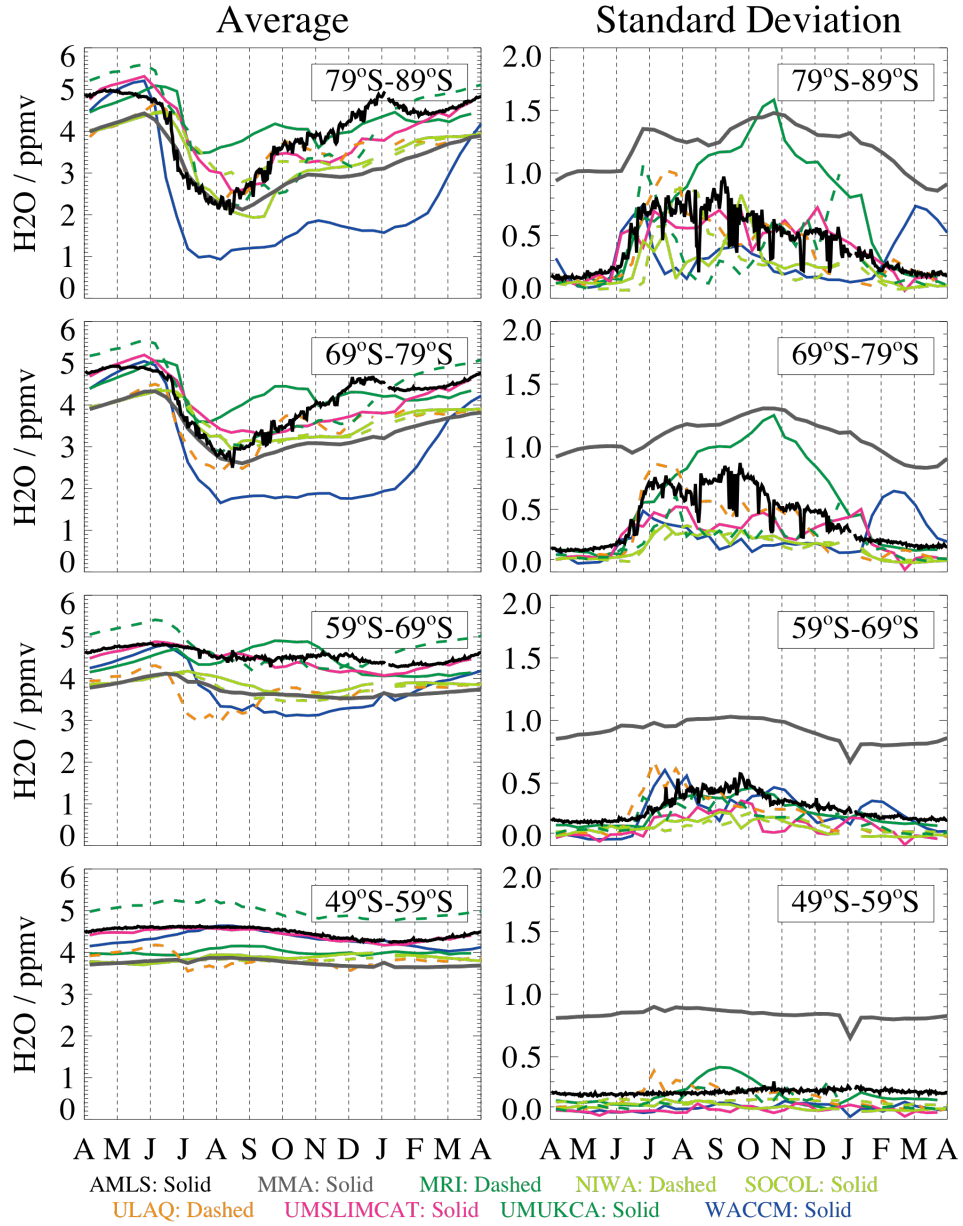
**Figure 6S-18:** As Figure 6S-17 but for HCl.

Southern Hemisphere at 500K  
H<sub>2</sub>O from CCM and Aura MLS Climatologies



151  
152 **Figure 6S-19a:** Left panels display variations in average H<sub>2</sub>O at 500K during the course  
153 of a year in 4 EqL bins, based on climatologies from Aura MLS (black, solid lines) and 7  
154 CCMs (with model sources shown in bottom legend). Right panels show the  
155 corresponding rms variability over the 5-year climatology, for each sampled day of year.  
156

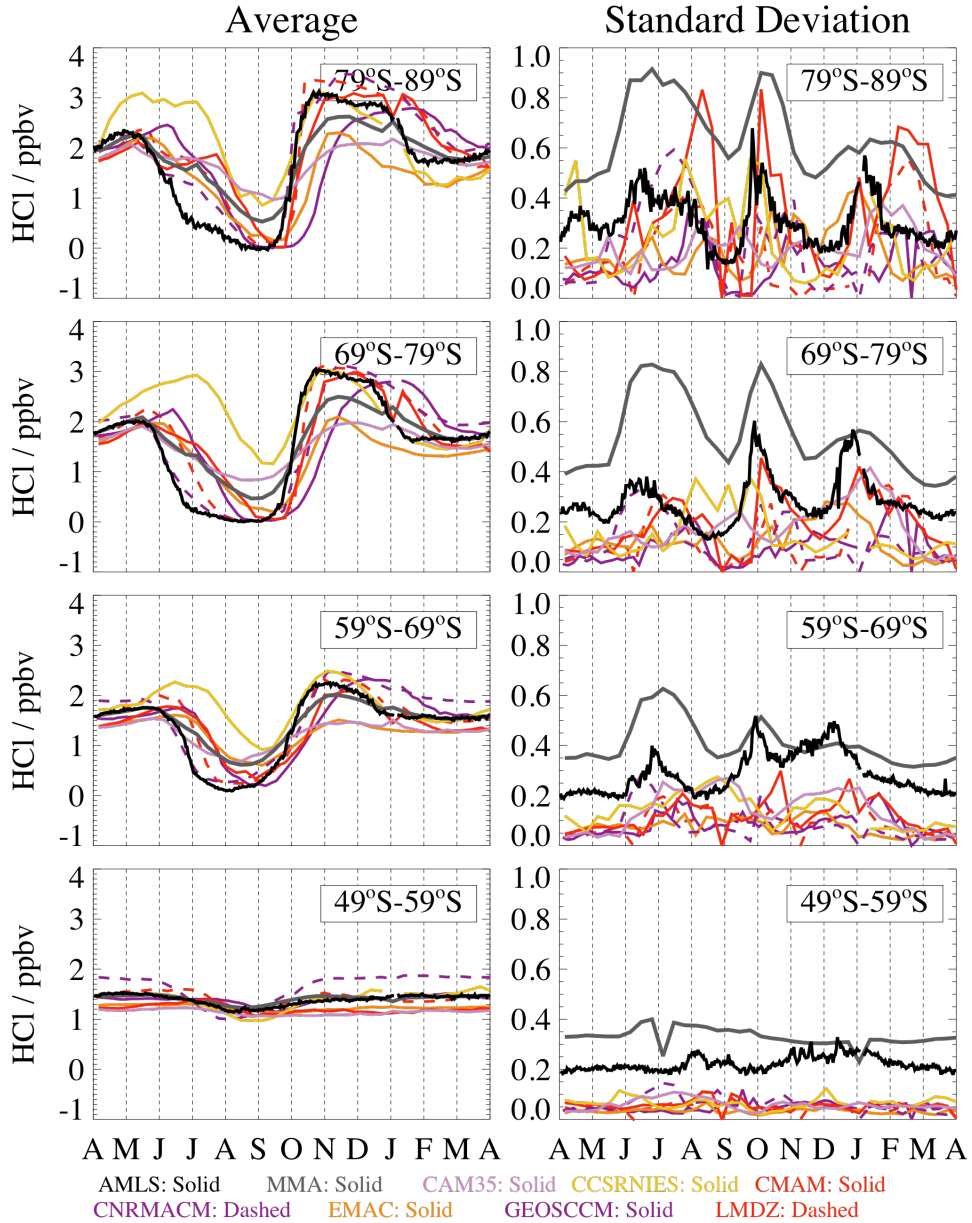
Southern Hemisphere at 500K  
H<sub>2</sub>O from CCM and Aura MLS Climatologies



157  
158  
159  
160

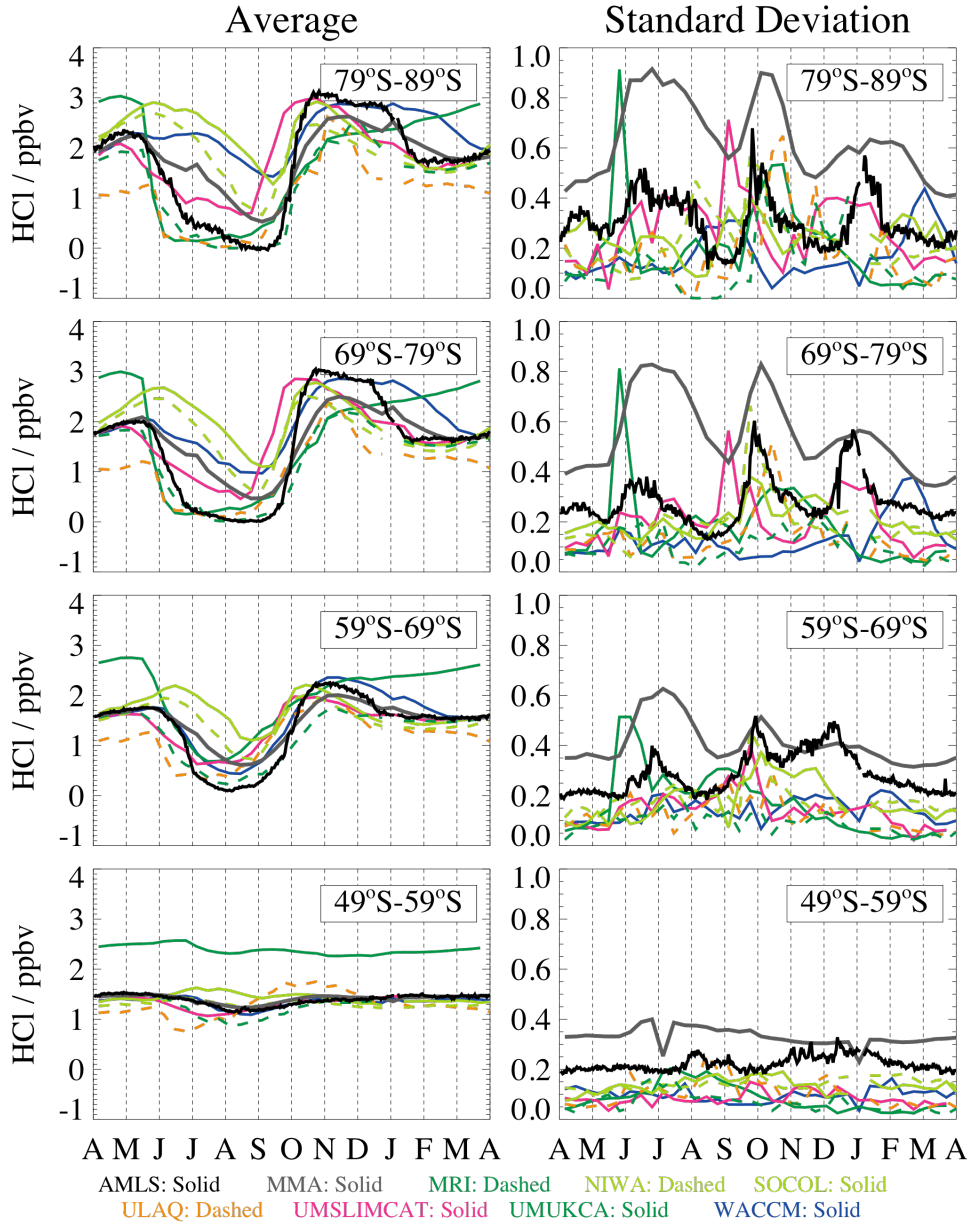
**Figure 6S-19b:** Same as Figure 6S-16a, but for Aura MLS H<sub>2</sub>O (and its rms variability) compared to the 7 other available CCM distributions of H<sub>2</sub>O versus time of year.

Southern Hemisphere at 500K  
HCl from CCM and Aura MLS Climatologies



161  
162 **Figure 6S-20a:** Left panels display variations in average HCl at 500K during the course  
163 of a year in 4 EqL bins, based on climatologies from Aura MLS (black, solid lines) and 7  
164 CCMs (with model sources shown in bottom legend). Right panels show the  
165 corresponding rms variability over the 5-year climatology, for each sampled day of year.  
166

Southern Hemisphere at 500K  
HCl from CCM and Aura MLS Climatologies



167  
168  
169  
170

**Figure 6S-20b:** Same as Figure 6S-20a, but for Aura MLS HCl (and its rms variability) compared to the 7 other available CCM distributions of HCl versus time of year.